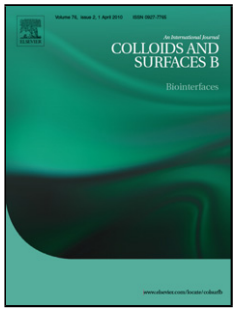

Title: Gallate-Induced Nanoparticle Uptake by Tumor Cells: Structure-Activity Relationships

Authors: Min-Chi Cheng, Yi-Ching Lu, Jender Wu, Yunn-Hwa Ma

PII: S0927-7765(19)30197-3
DOI: https://doi.org/10.1016/j.colsurfb.2019.03.048
Reference: COLSUB 10098

To appear in: *Colloids and Surfaces B: Biointerfaces*

Received date: 18 September 2018
Revised date: 15 March 2019
Accepted date: 21 March 2019

Please cite this article as: Cheng M-Chi, Lu Y-Ching, Wu J, Ma Y-Hwa, Gallate-Induced Nanoparticle Uptake by Tumor Cells: Structure-Activity Relationships, *Colloids and Surfaces B: Biointerfaces* (2019), https://doi.org/10.1016/j.colsurfb.2019.03.048

Gallate-Induced Nanoparticle Uptake by Tumor Cells: Structure-Activity Relationships

Min-Chi Cheng,[1]* Yi-Ching Lu,[2]* Jender Wu,[1#] Yunn-Hwa Ma[2,3#]

[1]School of Pharmacy, Taipei Medical University, 250 Wu-Hsing Street, Taipei 11031, Taiwan, ROC
[2]Department of Physiology and Pharmacology & Healthy Aging Research Center, Chang Gung University, Guishan, Taoyuan 33302, Taiwan, ROC
[3]Department of Neurology, Chang Gung Memorial Hospital, Guishan, Taoyuan 33305, Taiwan, ROC

Running title: Gallates enhance MNP-cell interactions

* Both authors contributed equally to this work.
# Correspondence and requests for reprints should be addressed to:
Yunn-Hwa Ma yhma@mail.cgu.edu.tw or
Jender Wu jd0332@tmu.edu.tw

Graphical abstract

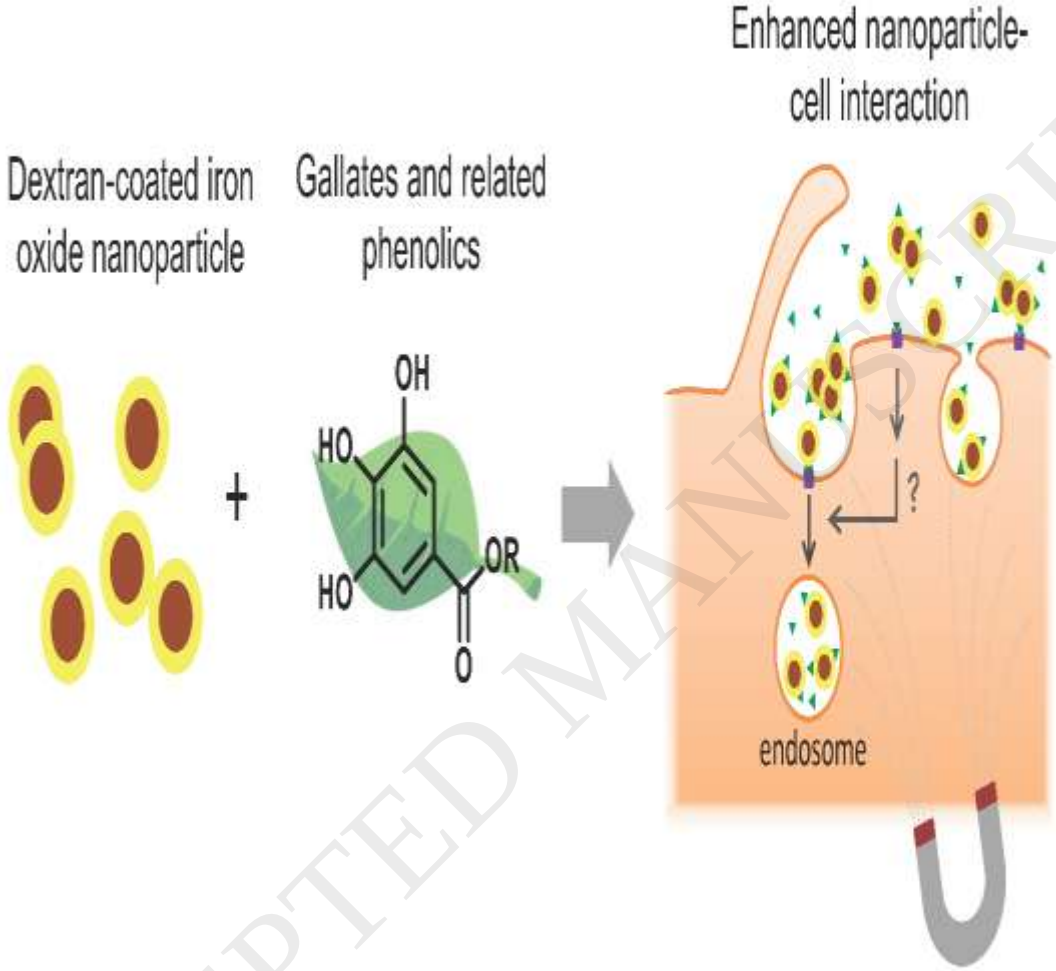

Highlights

- Co-incubation of gallates and MNPs enhanced MNP internalization by tumor cells.
- The galloyl moiety may be the pharmacophore of MNP-cell interaction enhancement.

- Two adjacent hydroxyl groups on the benzene ring are crucial for the enhancement.
- Methyl gallate and gallamide exerted most potent effects among derivatives studied.
- Magnetic force and gallates exerted a synergetic effect on cellular uptake of MNPs.

Abstract

How nanoparticles interact with biological systems determines whether they can be used in theranostic applications. It has been demonstrated that tea catechins, may enhance interactions of magnetic nanoparticles (MNPs) with tumor cells and the subsequent cellular internalization of MNPs. As part of the chemical structure of the major tea catechins, gallates are found in a variety of plants and thus food components. We asked whether the structure of gallate might act as a pharmacophore in the enhancement of the effects of MNP-cell interactions. Uptake of dextran-coated MNPs by glioma cells and cell-associated MNPs (MNP_{cell}) were respectively analyzed by confocal microscopy and a colorimetric iron assay. Co-incubation of MNPs and gallates, such as gallic acid and methyl gallate, induced a concentration-dependent increase in MNP_{cell}, which was associated with co-localization of internalized MNPs and lysosomes. An analysis of the structure-activity relationship (SAR) revealed that the galloyl moiety exerted the most prominent enhancement effects on MNP_{cell} which was further potentiated by the application of magnetic force; catechol coupled with a conjugated carboxylic acid side chain displayed comparable effects to gallate. Blockade or reduction in the number of hydroxyl groups rendered these compounds less effective, but without inducing cytotoxicity. The SAR results suggest that neighboring hydroxyl groups on the aromatic ring form an essential scaffold for the uptake effects; a similar SAR on antioxidant activities was also observed using a free radical-scavenging method. The results provide pivotal information for theranostic

applications of gallates by facilitating nanoparticle-cell interactions and nanoparticle internalization by tumor cells.

Key words: Gallic acid; Magnetic nanoparticle; Structure-activity relationship; Polyphenols

1. Introduction

Over the past few decades, intensive investigations on nanoparticles have brought about great potential applications ranging from chemistry, physics, and biotechnology to medicine. Biomedical applications of nanoparticles, particularly in the field of drug delivery, have garnered much attention and have been extensively studied [1-4]. Among various nanoparticles, magnetic nanoparticles (MNPs) are one of the most established drug delivery carriers. MNPs have a myriad of potential applications, including drug delivery for targeted therapy [4,5], gene delivery [2], contrast agents in magnetic resonance imaging [4-6], magnetic hyperthermia [3,5,7], biosensors[8], etc. MNPs are composed of a magnetite (Fe_3O_4) or maghemite (γ-Fe_2O_3) core and a polymeric coating, which may be designed to increase the particle stability/water dispersibility in physiological conditions and targeting effects *in vivo* [3,9]. Superparamagnetism, a unique characteristic of MNPs, allows MNPs to rapidly acquire or lose magnetic responsiveness in response to the presence or absence of an external magnetic field, respectively, thus achieving magneto-guidance.

In order to exert the intended effects of the active components, carriers have to get close to the target site and/or interact with the target on the cell membrane or inside the cell. Therefore, the efficiency of cellular uptake and membrane adsorption is critical and may affect the outcome of the therapy or diagnosis. In general, cellular uptake of nanoparticles is dependent on certain characteristics of the particles, including the size, shape, functional groups on the surface, etc. [9-11]. An external magnetic force may guide MNPs to a desired target site, improve accumulation in target tissues, and enhance their cellular uptake [12,13]. Magnetic targeting techniques were demonstrated to be feasible in preclinical studies for treating gliomas and breast cancer [5,14]. The surface charge is another factor that may modulate particle-cell interactions. It is generally considered that positively charged nanoparticles tend to interact with negatively charged components on cell membranes; such

electrostatic attraction facilitates more efficient internalization of cationic nanoparticles than neutral or negatively charged nanoparticles [10,15]. Many synthetic and natural polymers, such as dextran, have also been employed to modify the surface of MNPs to improve the diagnostic and therapeutic efficacies [3,6].

Phenolic acids are naturally occurring compounds in plants and are widely found in fruits, vegetables, and beverages. Phenolic acids are non-flavonoid polyphenolic compounds that can be further divided into two major groups, hydroxybenzoic acids and hydroxycinnamic acids [16]. Chemically, they are composed of at least one aromatic ring with one or more hydroxyl groups [17]. Gallic acid, which belongs to the hydroxybenzoic acid type, is one of the most important phenolic compounds. Gallic acid was proven to be effective against oxidative damage induced by superoxide, hydrogen peroxide, peroxyl, and non-radicals, which are often encountered in biological systems [18]. Due to their antioxidative properties, gallic acid and its ester derivatives have been used as additives or excipients in the pharmaceutical, cosmetic, and food industries [18,19]. Moreover, gallic acid and related derivatives were reported to exhibit a diverse range of bioactivities, such as antineoplastic, antimicrobial, anti-inflammatory [20], neuroprotective [18], chemopreventive, and lipid-regulatory effects [18,20]. Due to their inherent antioxidative ability, phenolic compounds are adopted as eco-friendly reducing and stabilizing agents in nanoparticle preparations. Gallic acid had been used to prepare silver and selenium nanoparticles [21-23]. Furthermore, gallic acid–nanoparticle conjugates showed diverse bioactivities. For example, gallic acid grafted onto chitosan inhibited linoleic acid autoxidation better than did free gallic acid [24]. Silica nanoparticles with gallic acid covalently bonded to the surface exerted antioxidant and free radical-scavenging effects [25]; MNPs functionalized with gallic acid also exhibit antioxidant and antimicrobial activities with good biocompatibility [26,27].

In our previous studies, we found that epigallocatechin-3-gallate (EGCG), the major catechin in green tea, can be adsorbed onto MNPs, thereby modifying the surface properties of

MNPs, enhancing MNP-cell interactions, and subsequently enhancing MNP uptake by glioma cells [28,29]. Other catechins, such as epicatechin and epigallocatecin, were also demonstrated to exert similar enhancing effects; it was therefore deduced that the catechin backbone structure may participate in facilitating MNP-cell interactions [28]. In many studies, the trihydroxyl structure on the B and D rings of EGCG were thought to contribute to the antioxidative activity and also many other biochemical activities [30]. A molecular dynamic study indicated that the gallate ester moiety in EGCG critically affected the affinity toward lipid bilayers [31]. Moreover, the galloyl moiety was previously found to be an anchor group that showed high binding affinity and strong absorption onto inorganic materials [32]. Hence, galloyl-containing compounds, such as gallic acid, are commonly employed as linker molecules to crosslink functional groups and nanoparticles, and those nanomaterials showed improved uptake efficiency compared to unmodified materials [33]; multivalent polygalloyl constructs were also reported to bind to the surface of intestinal cells [34,35]. It is anticipated that the galloyl moiety may play an important role in many biological interactions. Gallic acid and its derivatives have also been tested as chemotherapeutic agents and used in the construction of nanocomposites for targeted delivery and such nanocomposites were demonstrated high cellular uptake [36-38]; however, whether gallates facilitate the cellular uptake of nanoparticles has not been studied. Therefore, in this study, we hypothesized that the trihydroxy benzene structure may act as a pharmacophore in enhancing the cellular uptake of MNPs. Effects of different phenolic acid derivatives on MNP-cell interactions were studied.

2. Experimental Section

2.1. Materials Dextran-coated MNPs (nanomag®-D COOH; 250 nm) were purchased from micromodPartikel-technologie (Rostock, Germany); green fluorescent carboxymethyl-dextran-coated MNPs (nano-screen MAG-CMX; 200 nm) was purchased from Chemicell

(Berlin, Germany). Dulbecco's modified Eagle's medium (DMEM), minimum essential media (MEM), and trypsin-EDTA were purchased from Gibco BRL (Grand Island, NY). Penicillin/streptomycin/amphotericin B was purchased from Upstate (Lake Placid, NY). Fetal bovine serum (FBS), ammonium persulfate, potassium thiocyanate, caffeic acid, ferulic acid, hydrochloric acid, paraformaldehyde, 2,2-diphenyl-1-picrylhydrazyl (DPPH), and Cell Counting Kit-8 (CCK-8) were purchased from Sigma-Aldrich (St. Louis, MO). Lysotracker® and 4',6-diamidino-2-phenylindole (DAPI) were purchased from Invitrogen (Carlsbad, CA). Trimethoxybenzoic acid, protocatechuic acid, and α-resorcylic acid were purchased from TCI (Tokyo, Japan). Gallic acid monohydrate was from Janssen Chimica (Beerse, Belgium); gallamide (3,4,5-trihydroxybenzamide) was from Alfa Aesar (Heysham, Lancashire, UK); *p*-hydroxybenzoic acid was purchased from Merck (Darmstadt, Germany).

2.2. Synthesis Unless otherwise specified, all chemicals were of reagent grade and were used as received without further purification. The following compounds were synthesized and analyzed using a Bruker Fourier 300 NMR spectrometer or Bruker Avance DRX 500 NMR spectrometer (Bruker, Billerica, MA).

2.2.1 Methyl gallate (2) To a stirred suspension of gallic acid monohydrate (4.09 g, 21.7 mmol) in methanol (16 mL) at 0°C, thionyl chloride (2 mL, 27.6 mmol) was added dropwise. The mixture was heated under reflux for 3.5 h. The reaction mixture was then poured into a crushed ice bath. The resulting precipitate was filtered and washed thoroughly with water. The crude product was recrystallized from *n*-hexane-ethyl acetate to provide methyl gallate as a white crystal, mp 199~201°C [39]. ^{1}H NMR (300 MHz, CD_3OD) δ (ppm) 3.82 (s, 3H), 7.04 (s, 2H); ^{13}C NMR (125 MHz, CD_3OD) δ(ppm) 52.4, 110.2, 121.6, 139.9, 146.7, 169.2 (Figs. S1, S2).

2.2.2. Propyl gallate (3). To a stirred suspension of gallic acid monohydrate (0.30 g, 1.6 mmol) in 1-propanol (5 mL), thionyl chloride (0.8 mL, 11 mmol) was added dropwise. The mixture was heated under reflux for 5.5 h. The reaction mixture was poured into a crushed ice bath and

extracted three times with 70 mL of ethyl acetate. The combined organic layer was washed with water several times, dried over $MgSO_4$, and evaporated under reduced pressure. The crude product was recrystallized from aqueous ethanol to provide propyl gallate as a white crystal, mp 145~148°C. ^{1}H NMR (300 MHz, CD_3OD) δ(ppm) 1.03 (t, J = 7.5 Hz, 3H), 1.76 (m, 2H), 4.18 (t, J = 6.5 Hz, 2H), 7.05 (s, 2H)[40]; ^{13}C NMR (125 MHz, CD_3OD) δ(ppm) 11.0, 23.4, 67.4, 110.2, 121.9, 139.9, 146.6, 168.8 (Figs. S3, S4).

2.2.3. Dihydrocaffeic acid (10). In a hydrogenation bottle was placed 51.5 mg of 5% Pd/C and a solution of caffeic acid (0.5047 g, 2.8 mmol) in methanol (16 mL). Hydrogenation was performed in a Parr hydrogenation apparatus at a pressure of 26~35 psi for 3.5 h. The Pd/C was filtered off through a pad of celite, and the filtrate was evaporated under reduced pressure. The crude product was recrystallized from water to provide dihydrocaffeic acid as an off-white crystal, mp 138.5~140°C[41]. ^{1}H NMR (300 MHz, CD_3OD) δ(ppm) 2.51 (t, J = 7.8 Hz, 2H), 2.76 (t, J = 7.8 Hz, 2H), 6.52 (dd, J = 7.8, 2.2 Hz, 1H), 6.65 (d, J = 2.2 Hz, 1H), 6.66 (d, J = 7.8 Hz, 1H); ^{13}C NMR (125 MHz, CD_3OD) δ(ppm) 31.7, 37.4, 116.5, 116.6, 120.6, 133.9, 144.7, 146.3, 177.2 (Figs. S5, S6).

2.3. Cell culture LN-229 cells, human glioma cells, were cultured in DMEM; whereas HeLa cells, human cervical cancer cells, were cultured in MEM. Both media were supplemented with 10% FBS and a 1% penicillin/streptomycin/amphotericin B solution. Cells were maintained in a 37°C incubator supplied with 5% CO_2 and subcultured every 3~4 days.

2.4. Determination of cell-associated MNPs ($MNPs_{cell}$) LN-229 or HeLa cells were seeded and grown in 24-well plates. After attaining 80%~90% confluence, cells were exposed to MNPs (100 μg/mL; 26.32 μg/cm^2) and phenolic compounds (10 or 30 μM) in the presence or absence of an NdFeB magnet underneath the plate for 24 h. In some experiments, cells were equilibrated at 4°C for 20 min, followed by an additional 2 h incubation with MNPs at 4°C in the absence and presence of the magnet. A home-made magnetic plate with 24 pieces of a cylindrical NdFeB magnet were used to provide a magnetic field of 3.4 kG at the center of

each well [12]. For the group without a magnet during incubation with MNPs, the magnetic plate was placed underneath the culture plates for 5 min after MNP administration to ensure MNP sedimentation at the beginning of incubation. Cells were then washed twice with phosphate-buffered saline (PBS) and trypsinized prior to colorimetric quantification. The cell pellet containing MNP_{cell} was treated with 10% hydrochloric acid at 55°C for 4 h, followed by the addition of an ammonium persulfate (1 mg/mL) and potassium thiocyanate solution (1 M). The amount of cell-associated iron was determined with a VICTOR3 Multilabel Plate Reader (PerkinElmer, Waltham, MA) at OD_{490}. A calibration curve was prepared under identical conditions.

2.5. Confocal microscopy LN-229 cells were seeded onto poly-lysine-coated coverslips 18 h before the experiments. Cells were incubated with green fluorescent MNPs with a carboxylmethyl-dextran coating (nano-screenMAG-CMX; 100 µg/mL; 26.32 µg/cm^2) and methyl gallate (30 µM) at 37 °C for 2 h in the presence of an NdFeB magnet underneath the culture plate. Cells were then washed twice with PBS and then incubated with Lysotracker® (0.125 µM) for 30 min to stain lysosomes. Cells were than washed with PBS and fixed with 4% paraformaldehyde for 20 min at room temperature. Cells were counterstained with DAPI and imaged with a Zeiss LSM 510 Meta laser confocal microscope system (Carl Zeiss, Jena, Germany) equipped with a 100×/1.4 oil immersion objective lens. Image processing and analysis of fluorescent MNPs colocalized with cells were performed using Fiji Image J.

2.6. Antioxidant activity assay A stable and commercially available organic nitrogen radical reagent, DPPH, was used to determine the scavenging activity of gallate derivatives. Briefly, 6 µL of 2% DMSO containing 0.1, 1, or 5 mM of gallate derivatives was mixed with 194 µL of DPPH in ethanol (0.1 mM) to a final gallate derivative concentration of 3, 30, or 150 µM, respectively. Samples were reacted at room temperature for 20 min, followed by

determination of OD_{517}.The free radical-scavenging activity was calculated by subtracting the decrease of DPPH absorption induced by gallate compounds to that of the vehicle control.

2.7. Cellular toxicity assay The cytotoxicities of gallate compounds toward LN-229 cells were measured using a CCK-8 kit according to the manufacturer's instructions. Briefly, LN-229 cells were cultured in a 24-well plate to 80%~90% confluence before incubation with gallate compounds (10 or 30 μM) or in combination with MNPs (100 μg/mL; 26.32 μg/cm^2). After administration of MNPs, a magnet was placed underneath for 5 min or 2 h. Then, cells were washed with PBS and incubated with medium containing a 10% CCK-8 solution for additional 1 h. The absorbance of each sample at 450 nm (OD_{450}) was determined with a microplate reader (VICTOR3 Multilabel Plate Reader, PerkinElmer, Waltham, MA). The percentage of viability was calculated as follows: (viable cells) % = (OD of the drug-treated sample / OD of the untreated sample) × 100.

2.8. Statistical analysis Results are expressed as the mean ± standard error (SE). Statistical evaluation of the data was performed with Student's *t*-test for simple comparisons between two values when appropriate. For multiple comparisons, results were analyzed by a 2-way analysis of variance (ANOVA) followed by Duncan's *post-hoc* test. A value of $p<0.05$ was considered statistically significant.

3. Results

3.1. Gallates enhanced tumor cell-MNP interactions

Based on our previous study that EGCG exerted an enhancing effect on MNP uptake, effects of gallic acid and methyl gallate on MNP_{cell} were measured to determine whether the gallate moiety of EGCG may be the key structure that enhances MNP internalization. Figure 1 depicts that both gallic acid (Fig. 1A, B) and methyl gallate (Fig. 1C, D) induced concentration-dependent increments in cell-associated MNPs (MNP_{cell}) with or without a magnet underneath the cells, whereas the magnet significantly enhanced MNP_{cell} in all conditions studied.

Compared to the vehicle group, gallic acid at a concentration of as low as 6 μM induced a significant increase in LN-229 cell-associated MNPs both with and without the magnet; at 50 μM, gallic acid increased MNP_{cell} by 5.4- and 3.9-fold in the absence and presence of the magnet, respectively (Fig. 1A). Similar effects were observed in HeLa cells, where gallic acid at 10 μM increased MNP_{cell} by 1.8- and 1.9-fold in the absence and presence of the magnet, respectively (Fig. 1B).

Methyl gallate, a methyl ester of gallic acid, also enhanced MNP_{cell} in a concentration-dependent manner both with and without the magnet (Fig. 1C). In LN-229 cells, methyl gallate increased MNP_{cell} by 1.4-fold at 10 μM and further increased MNP_{cell} by 4.5-fold at 50 μM in the absence of the magnet (Fig. 1C). With the magnet underneath LN-229 cells, methyl gallate increased MNP_{cell} by 2.1-fold at 10 μM and 2.9-fold at 50 μM (Fig. 1C). Similar synergetic effects were observed in HeLa cells, where methyl gallate at 10 μM induced a 0.6- *vs.* 1.0-fold increase of MNP_{cell} in the absence and presence of the magnet (Fig. 1D), respectively.

3.2. Methyl gallate enhanced MNP internalization

To determine whether gallate compound-induced increases in MNP_{cell} were associated with increased MNP internalization, green fluorescent CMX-MNPs were incubated with LN-229 cells in the presence of methyl gallate. Figure 2 depicts the representative distribution of MNP_{cell} relative to those of lysosomes and nuclei. Compared to the vehicle (Fig. 2A), methyl gallate (30 μM; 2 h) greatly increased the internalization of MNPs (Fig. 2B). Green fluorescent signals were distributed outside nuclei in blue, suggesting that MNPs were internalized in the cytoplasm but not in nuclei. In addition, co-localization of internalized MNPs with lysosomes was observed in the cytoplasm (Fig. 2B), suggesting that MNP internalization was predominantly mediated by endocytosis. The overlap coefficient, Mander's coefficients, of MNPs relative to lysosomes were 0.51 ± 0.08 (n = 6) and 0.65 ± 0.03 (n = 8) in the absence and presence of methyl gallate, respectively, suggesting an increase in MNPs transported into lysosomes in the cells.

Furthermore, incubation of gallates and MNPs with LN-229 cells at 4°C significantly reduced MNP_{cell} in all groups studied, suggesting that endocytosis was inhibited by a low temperature (Fig. 2C). Compared to 37°C, MNP uptake at 4°C reduced to 42% and 43% in the absence and presence of the magnet, respectively. At 4°C, gallic acid or methyl gallate enhanced MNP_{cell} by 1.9- or 1.4-fold without the magnet and 0.6- or 0.4-fold with the magnet, respectively. These results suggested that the magnetic force- and gallate compound-induced increases in MNP_{cell} might not only occur by enhancing MNP internalization but also by MNP-cell interactions.

3.3. Structural features of the galloyl moiety in relation to uptake enhancement

We surmised that gallic acid (**1**) may be a pharmacophore in the enhancement effect of nanoparticle-cell interactions, and related gallate derivatives (**2~4**, **8**) and congeners (**5~7**, **9~11**) were selected to evaluate the effects on MNP_{cell} (Fig. 3). LN-229 cells were incubated with compounds **1**~**11** at 10 or 30 μM with MNPs for 24 h followed by a quantitative analysis of MNP_{cell} (Fig. 4). Compared to the corresponding vehicle group, gallic acid (**1**) and derivatives with a modified side chain (**2~4**) at 10 μM enhanced MNP_{cell} by 1.9~4.0-fold in Mag (-) and 2.5~3.9-fold in Mag (+), respectively (Fig. 4A). At 30 μM, gallic acid and its derivatives (**1~4**) increased MNP_{cell} by 2.8~9.5-fold in Mag (-) and 2.9~5.0-fold in Mag (+), respectively (Fig. 4C).

To determine whether the locations and numbers of hydroxyl groups on the benzene ring of gallates may be pivotal in the enhancing effects on MNP_{cell}, a gallate derivative (**8**) and three congeners (**5~7**) were tested. Compared to gallic acid, protocatechuic acid (**5**) reduced MNP_{cell} to 35%~36% and 55%~56%, respectively, in the absence and presence of the magnet at the concentrations studied (Fig. 4A, C). Furthermore, *p*-hydroxybenzoic acid (**6**), α-resorcylic acid (**7**), and trimethoxybenzoic acid (**8**) exerted no effects on MNP_{cell} regardless of the absence or presence of the magnet.

In addition to benzoic acid-based phenols, we also examined cinnamic acid-based phenol compounds (**9**~**11**) to gain insights into molecular features associated with the enhancing effect. At 10 μM, caffeic acid (**9**) enhanced MNP_{cell} by 1.5- and 2.3-fold without and with the magnet (Fig. 4B), respectively. At 30 μM, caffeic acid produced an approximately 4-fold MNP_{cell} enhancement either with or without the magnet (Fig. 4D), suggesting that caffeic acid (**9**) exerted a concentration-dependent increase in MNP_{cell} with or without the magnet. Compared to caffeic acid (**9**), dihydrocaffeic acid (**10**) reduced MNP_{cell} to 53%~72% and 70%~71% of that of caffeic acid in the absence and presence of the magnet (Fig. 4B, D), respectively. In addition, ferulic acid (**11**) exerted no effect on MNP_{cell} in all condition studied compared to the vehicle (**v**) groups (Fig. 4B, D).

3.4 Antioxidant activity

Gallic acid and its derivatives are often employed as antioxidants in food [42,43], therefore, we asked whether the pattern of the enhancement effect of these compounds on MNP_{cell} might be associated with their antioxidant activities by determining their free radical-scavenging activity. Figure 5 demonstrates antioxidant activities of compounds **1~11** according to a DPPH-scavenging assay. Gallic acid (**1**), methyl gallate (**2**), propyl gallate (**3**), and gallamide (**4**) exerted similar concentration-dependent antioxidant activities by scavenging 19%~26% of free radicals at 0.1 mM and 74%~80% of free radicals at 5 mM. Compared to gallic acid and related derivatives with similar structures (**1~4**), activities of protocatechuic acid (**5**) were reduced to 0.4~0.6-fold at the concentrations studied. In addition, *p*-hydroxybenzoic acid (**6**), α-resorcylic acid (**7**), and trimethoxybenzoic acid (**8**) exhibited no scavenging efficiency against DPPH (3%~7%) at all concentrations studied (Fig. 5A). Scavenging efficiencies of cinnamic acid-based phenols, such as caffeic acid (**9**) and dihydrocaffeic acid (**10**), were less than those of the gallic derivatives (**1~4**) described above. The scavenging efficiencies against DPPH of caffeic acid (**9**) and dihydrocaffeic acid (**10**) were 10.9% ± 0.88% and 17.3% ± 0.46% at 0.1 mM,

whereas the efficiencies rose to 60.4% ± 3.52% and 73.1% ± 2.64% at 5 mM, respectively. Ferulic acid (**11**) exerted lower antioxidant activity at most concentrations studied (Fig. 5B).

3.5. Cell Viability

In order to determine whether variations in MNP_{cell} were due to cellular toxicity induced by some gallate derivatives, a cell viability assay was conducted on LN-229 cells exposed to these compounds. After a 2-h incubation with gallate derivatives, no changes in cell viability were observed even at 30 μM of gallates in the absence (Fig. 6A) or presence (Fig. 6B) of MNPs. These results implied that the concentrations of these compounds used in this study may have been below the threshold for inducing cytotoxicity.

4. Discussion

Our previous study demonstrated equivalent enhancement of tea catechins on MNP uptake by glioma cells, suggesting that the galloyl or catechol moiety may play a critical role in the enhancement of MNP-cell interactions [28]. In this study, eleven phenolic acids with varying number and position of phenol groups were prepared and tested for their MNP uptake enhancement activities by a colorimetric iron assay. The results demonstrated that galloyl and catechol functionality are vital for the enhancement of cellular uptake of MNPs, and methylation of galloyl moiety to produce trimethoxybenzoic acid, aiming at the blockade of hydrogen bonds, greatly reduced MNP-cell interactions, suggesting the importance of the free phenolic hydroxyl components in the structure. This finding is consistent with a previous report that the galloyl moiety may play an important role in many of the biological activities of catechins and other polyphenol compounds, including antiproliferative effects and radical-scavenging activities [42].

Previous studies also demonstrated that the catecholic functionality of 3,4-dihydroxyphenylalanine (DOPA) or dopamine in marine mussels may afford adhesive and

anchoring properties, which can bind strongly to various inorganic and organic surfaces or increase absorption, binding, and adhesion capabilities to different surfaces and tissues [44,45]. Since gallic acid and dopamine share a similar hydroxyl groups substituted benzene structure, it is anticipated that both galloyl and catechol may possess similar properties and mechanisms toward the cell membrane adhesion by formation of non-specific hydrogen bonds with polar groups present on cell membranes. Furthermore, galloyl and catechol may be oxidized to form *o*-quinones, which can undergo Michael addition or Schiff base reaction with nucleophilic groups, and subsequently react with amino and thiol groups of polysaccharides and proteins on cell membranes [46]. In addition, high affinity between the galloyl moiety of catechins and phosphatidylcholine on cell membranes by cation-π interactions was reported [47]. These combined interactions may give rise to the enhancing effects on MNP-cell interactions of gallate derivatives.

The uptake of MNPs was greatly attenuated at 4°C (Fig. 2), suggesting involvement of endocytosis in the enhancement effects of gallates at 37°C. In addition, the synergetic effects of gallates and the magnet observed in the current study are consistent with previous findings with EGCG [28]. Our results support a role of energy-dependent endocytosis in the synergetic effects. The enhanced MNP_{cell} observed in LN-229 and HeLa cells suggest that such effects of gallates may occur in various cancer cells.

According to the SAR results, ester and amide derivatives of gallic acid exerted notable enhancement effects among the tested compounds. Gallic acid (**1**), methyl gallate (**2**), propyl gallate (**3**), and gallamide (**4**) exerted similar concentration-dependent effects on MNP internalization and antioxidant activity. However, replacing the trihydroxyl groups with methoxy groups, i.e., trimethoxybenzoic acid (**8**), rendered the compound nearly inactive, suggesting that the galloyl moiety is crucial. In addition, protocatechuic acid (**5**), with one hydroxyl group at the *meta*-position removed from the benzene ring of gallic acid, exhibited significantly attenuated effects on MNP_{cell} and also the antioxidant activity compared to gallic

acid and related derivatives (**1~4**). Mono-hydroxyl substitution at the *para*-position (**6**) or di-hydroxyl substitution at the *meta*-position (**7**) of the carboxylic group also resulted in complete loss of both activities studied under all conditions (Figs. 4, 5). These results suggest that radical-scavenging activities and enhancement effects depend on the number and also the distribution of hydroxyl groups on the aromatic rings [42]. Antioxidant activities of phenolics are often estimated by bond dissociation enthalpy (BDE). Lower BDE value indicates a higher phenolic hydrogen atom donating ability by cleaving the O–H bond, and might associated with the easier formation of quinone [48]. The formed quinone may react with the nucleophilic groups on cell membrane and thus increase the interaction [46]. More hydroxyl groups substituted on the aromatic ring tend to decrease the O–H BDEs. The BDE values of tested phenolics in ascending order are propyl gallate (69.6 kcal/mol), gallic acid (70.2), protochuic acid (75.5), and p-hydroxybenzoic acid (84.7) [49]. This tendency is correlated to the uptake enhancement effects. In contrast, N-acetylcysteine, a commonly used antioxidant, did not show the uptake enhancement effect [28] due to a distinct antioxidant mechanism.

It was noted that protocatechuic acid (**5**) still increased MNP_{cell} with the magnet, suggesting that replacement of the galloyl moiety with the catechol structure on benzoic acid may still exert a partial enhancement effect on MNP_{cell} in the presence of the magnet. Therefore, phenolic acids with a catechol structure are worthy of further evaluation. The cinnamic acid-based phenol compounds, caffeic acid (**9**) and dihydrocaffeic acid (**10**), which have a conjugated carboxylic acid and catechol moiety, also exhibited concentration-dependent enhancing effects (Fig. 4B, D). At 10 μM, caffeic acid (**9**) enhanced MNP_{cell} in the presence but not in the absence of the magnet, suggesting that caffeic acid (**9**) may exert a synergetic effect similar to protocatechuic acid (**5**) due to the catechol structure. Dihydrocaffeic acid (**10**), in which the conjugated double bond at the side chain of caffeic acid is replaced with a single bond, hindered the interaction of MNPs with cells compared to caffeic acid (**9**). Ferulic acid (**11**), with methylation of the *meta*-hydroxyl group on caffeic acid, showed no uptake

enhancement effect at both concentrations studied compared to the vehicle (**v**) groups (Fig. 4B, D). These results suggested that at least two adjacent hydroxyl groups on the benzene ring, such as the catechol structure, are essential for the enhancement of MNP_{cell}. Additionally, the conjugated double bond on the side chain may facilitate such an effect.

In the current study, gallate derivatives (**2**~**4**) showed significantly higher internalization effects than did the parent compound (**1**), suggesting that the side chain of gallate may modulate the enhancing effect of gallates on MNP_{cell}. In a physiological solution, gallic acid ionizes to become a carboxylate anion, which has strong ionic interactions and serves as a strong hydrogen bond acceptor and donor. The ester group can only act as a hydrogen bond acceptor but cannot form an anion. Furthermore, the amide side chain does not form an anion in physiological conditions, and the hydrogen bond strength is weaker than that of carboxylic acid. Such a chemical transformation implies that the formation of hydrogen bonds and ionic bonds of the side chains may modulate the interaction among gallates, nanoparticles, and plasma membranes; however, the detailed surface interaction remains to be defined.

Bai et al. reported that polymeric organic nanoparticles with more lipophilic surface modifications entered cells more easily [50]. Replacement of the carboxylic acid group with an ester group increased the hydrophobicity of the molecules, which was associated with a higher logarithm of the octanol/water partition coefficient, log *P* [51]. Methyl gallate (**2**; log *P* = 0.9) and propyl gallate (**3**; log *P* = 1.8) exhibited higher log *P* values than gallic acid (**1**; log *P* = 0.7), which was also in line with the current results that higher hydrophobicity may increase the interaction of MNP-gallate conjugates with membranes. However, gallamide (**4**) is more hydrophilic with a much lower log *P* value (0), but a greater enhancing effect than gallic acid (**1**), indicating lipophilicity might not be a dominant parameter. These results suggested that both ester and amide modifications of the galloyl structure may facilitate MNP-cell interactions.

Our results demonstrated that the enhancing effects on MNP_{cell} are highly dependent on the structure of gallate derivatives. The number and arrangement of phenolic hydroxyl groups

seems to be critical structural features. Other than the versatile adhesive/anchoring properties of the galloyl or catechol structure, it is likely that a specific binding site, or a receptor, on the plasma membrane may mediate the enhancing effects of gallate derivatives to enhance nanoparticle-cell interactions. Previous studies reported that gallate may bind to G protein-coupled receptor 35 (GPR35) to induce anti-inflammatory effects [52]. Although there is no direct evidence suggesting the participation of GPR35 in endocytosis, we cannot rule out the possibility that the effects of gallate on MNP_{cell} might be mediated by receptor activation-induced signaling.

5. Conclusions

In the present study, we demonstrated a feasible application of combining gallate derivatives and MNPs for a targeted delivery system. A simple mix of gallic acid or methyl gallate with MNPs provided higher internalization compared to vehicle groups in LN-229 and HeLa cells. Further study of structure-activity relationships showed that the galloyl moiety enhanced MNP-cell interactions most prominently, while the catechol structure along with a conjugate carboxylic acid also showed comparable effects. Use of a magnetic field further facilitated particle internalization, suggesting a synergetic effect of phenolic acids and magnetic forces. An antioxidant assay displayed a similar pattern of activities to the enhancing effects, implying that enhancement of the uptake of MNPs and antioxidation may arise from common structural features. Such structure-activity relationships cannot be interpreted by cytotoxicity of the tested compounds with or without MNP conjugates at the concentrations tested. Co-administration of gallates and nanocarriers may be a potential strategy to enhance tumor cell-nanoparticle interactions, and thus improve cancer diagnosis and targeted therapy. Whether gallates can enhance nanoparticles with different coatings remains to be determined;

nevertheless, gallates may serve as a platform for further modifications for versatile applications.

Acknowledgements

We thank the Ministry of Science and Technology of the Republic of China (NSC 101-2320-B-182-038- and MOST 106-2320-B-182-002-), Chang Gung Memorial Hospital (CMRPD1D0231 and BMRP432), and the Ministry of Education of Taiwan (EMRPD1F0261) for funding support.

References

[1] S. Parveen, R. Misra, S.K. Sahoo, Nanoparticles: a boon to drug delivery, therapeutics, diagnostics and imaging, Nanomedicine, 8 (2012) 147-166.

[2] X.J. Loh, T.C. Lee, Q. Dou, G.R. Deen, Utilising inorganic nanocarriers for gene delivery, Biomater Sci, 4 (2016) 70-86.

[3] W. Wu, Z. Wu, T. Yu, C. Jiang, W.S. Kim, Recent progress on magnetic iron oxide nanoparticles: synthesis, surface functional strategies and biomedical applications, Sci Technol Adv Mater, 16 (2015) 023501.

[4] L.H. Reddy, J.L. Arias, J. Nicolas, P. Couvreur, Magnetic nanoparticles: design and characterization, toxicity and biocompatibility, pharmaceutical and biomedical applications, Chem Rev, 112 (2012) 5818-5878.

[5] R.A. Revia, M. Zhang, Magnetite nanoparticles for cancer diagnosis, treatment, and treatment monitoring: recent advances, Mater Today (Kidlington), 19 (2016) 157-168.

[6] Y.X. Wang, Superparamagnetic iron oxide based MRI contrast agents: current status of clinical application, Quant Imaging Med Surg, 1 (2011) 35-40.

[7] M. Banobre-Lopez, A. Teijeiro, J. Rivas, Magnetic nanoparticle-based hyperthermia for cancer treatment, Rep Pract Oncol Radiother, 18 (2013) 397-400.

[8] M. Hasanzadeh, N. Shadjou, M. de la Guardia, Iron and iron-oxide magnetic nanoparticles as signal-amplification elements in electrochemical biosensing, Trac-Trend Anal Chem, 72 (2015) 1-9.

[9] E. Amstad, M. Textor, E. Reimhult, Stabilization and functionalization of iron oxide nanoparticles for biomedical applications, Nanoscale, 3 (2011) 2819-2843.

[10] A. Albanese, P.S. Tang, W.C. Chan, The effect of nanoparticle size, shape, and surface chemistry on biological systems, Annu Rev Biomed Eng, 14 (2012) 1-16.

[11] G.Y. Tonga, K. Saha, V.M. Rotello, 25th anniversary article: Interfacing nanoparticles and biology: new strategies for biomedicine, Adv Mater, 26 (2014) 359-370.

[12] Y.C. Lu, F.Y. Chang, S.J. Tu, J.P. Chen, Y.H. Ma, Cellular uptake of magnetite nanoparticles enhanced by NdFeB magnets in staggered arrangement, J Magn Magn Mater, 427 (2017) 71-80.

[13] J. Huang, Y. Li, A. Orza, Q. Lu, P. Guo, L. Wang, L. Yang, H. Mao, Magnetic nanoparticle facilitated drug delivery for cancer therapy with targeted and image-guided approaches, Adv Funct Mater, 26 (2016) 3818-3836.

[14] M.F. de Paula Aguiar, J.B. Mamani, T.K. Felix, R.F. dos Reis, H.R. da Silva, P. Nucci Leopoldo, P. Nucci-da-Silva Mariana, F. Gamarra Lionel, Magnetic targeting with superparamagnetic iron oxide nanoparticles for in vivo glioma, Nanotechnol Rev, 6 (2017) 449-472.

[15] T. Mizuhara, D.F. Moyano, V.M. Rotello, Using the power of organic synthesis for engineering the interactions of nanoparticles with biological systems, Nano Today, 11 (2016) 31-40.

[16] R. Tsao, Chemistry and biochemistry of dietary polyphenols, Nutrients, 2 (2010) 1231-1246.

[17] R.J. Robbins, Phenolic acids in foods: an overview of analytical methodology, J Agric Food Chem, 51 (2003) 2866-2887.

[18] B. Badhani, N. Sharma, R. Kakkar, Gallic acid: a versatile antioxidant with promising therapeutic and industrial applications, RSC Adv, 5 (2015) 27540-27557.

[19] C. Locatelli, F.B. Filippin-Monteiro, T.B. Creczynski-Pasa, Alkyl esters of gallic acid as anticancer agents: a review, Eur J Med Chem, 60 (2013) 233-239.

[20] S. Choubey, L.R. Varughese, V. Kumar, V. Beniwal, Medicinal importance of gallic acid and its ester derivatives: a patent review, Pharm Pat Anal, 4 (2015) 305-315.

[21] D. Li, Z.J. Liu, Y. Yuan, Y.W. Liu, F.L. Niu, Green synthesis of gallic acid-coated silver nanoparticles with high antimicrobial activity and low cytotoxicity to normal cells, Process Biochem, 50 (2015) 357-366.

[22] F. Martinez-Gutierrez, P.L. Olive, A. Banuelos, E. Orrantia, N. Nino, E.M. Sanchez, F. Ruiz, H. Bach, Y. Av-Gay, Synthesis, characterization, and evaluation of antimicrobial and cytotoxic effect of silver and titanium nanoparticles, Nanomedicine, 6 (2010) 681-688.

[23] A.K. Mittal, S. Kumar, U.C. Banerjee, Quercetin and gallic acid mediated synthesis of bimetallic (silver and selenium) nanoparticles and their antitumor and antimicrobial potential, J Colloid Interface Sci, 431 (2014) 194-199.

[24] M. Xie, B. Hu, Y. Wang, X. Zeng, Grafting of gallic acid onto chitosan enhances antioxidant activities and alters rheological properties of the copolymer, J Agric Food Chem, 62 (2014) 9128-9136.

[25] Y. Deligiannakis, G.A. Sotiriou, S.E. Pratsinis, Antioxidant and antiradical SiO_2 nanoparticles covalently functionalized with gallic acid, ACS Appl Mater Interfaces, 4 (2012) 6609-6617.

[26] C.J. Katalin Farkas, Hemocompatibility and biomedical potential of poly(gallic acid) coated iron oxide nanoparticles for theranostic use, J Nanomed Nanotechnol, 06 (2015) 252-258.

[27] S.T. Shah, A.Y. W, O. Saad, K. Simarani, Z. Chowdhury, A.A. A, L.A. Al-Ani, Surface functionalization of iron oxide nanoparticles with gallic acid as potential antioxidant and antimicrobial agents, Nanomaterials (Basel), 7 (2017) E306.

[28] Y.C. Lu, P.C. Luo, C.W. Huang, Y.L. Leu, T.H. Wang, K.C. Wei, H.E. Wang, Y.H. Ma, Augmented cellular uptake of nanoparticles using tea catechins: effect of surface modification on nanoparticle-cell interaction, Nanoscale, 6 (2014) 10297-10306.

[29] W.X. Siow, Y.-T. Chang, M. Babič, Y.-C. Lu, D. Horák, Y.-H. Ma, Interaction of poly-L-lysine coating and heparan sulfate proteoglycan on magnetic nanoparticle uptake by tumor cells, Int J Nanomedicine, 13 (2018) 1693-1706.

[30] C.S. Yang, X. Wang, G. Lu, S.C. Picinich, Cancer prevention by tea: animal studies, molecular mechanisms and human relevance, Nat Rev Cancer, 9 (2009) 429-439.

[31] T.W. Sirk, E.F. Brown, A.K. Sum, M. Friedman, Molecular dynamics study on the biophysical interactions of seven green tea catechins with lipid bilayers of cell membranes, J Agric Food Chem, 56 (2008) 7750-7758.

[32] M.S. Ata, Y. Liu, I. Zhitomirsky, A review of new methods of surface chemical modification, dispersion and electrophoretic deposition of metal oxide particles, RSC Adv, 4 (2014) 22716-22732.

[33] E. Amstad, S. Zurcher, A. Mashaghi, J.Y. Wong, M. Textor, E. Reimhult, Surface functionalization of single superparamagnetic iron oxide nanoparticles for targeted magnetic resonance imaging, Small, 5 (2009) 1334-1342.

[34] C. Hamashin, L. Spindler, S. Russell, A. Schink, I. Lambkin, D. O'Mahony, R. Houghten, C. Pinilla, Identification of novel small-molecule Ulex europaeus I mimetics for targeted drug delivery, Bioorg Med Chem, 11 (2003) 4991-4997.

[35] S. Misumi, M. Masuyama, N. Takamune, D. Nakayama, R. Mitsumata, H. Matsumoto, N. Urata, Y. Takahashi, A. Muneoka, T. Sukamoto, K. Fukuzaki, S. Shoji, Targeted delivery of immunogen to primate m cells with tetragalloyl lysine dendrimer, J Immunol, 182 (2009) 6061-6070.

[36] S. Komenek, U. Luesakul, S. Ekgasit, T. Vilaivan, N. Praphairaksit, S. Puthong, N. Muangsin, Nanogold-gallate chitosan-targeted pulmonary delivery for treatment of lung cancer, AAPS PharmSciTech, 18 (2017) 1104-1115.

[37] P.E. Feuser, J.M. Arevalo, E.L. Junior, G.R. Rossi, E. da Silva Trindade, M.E. Rocha, A.V. Jacques, E. Ricci-Junior, M.C. Santos-Silva, C. Sayer, P.H. de Araujo, Increased cellular

uptake of lauryl gallate loaded in superparamagnetic poly(methyl methacrylate) nanoparticles due to surface modification with folic acid, J Mater Sci Mater Med, 27 (2016) 185-199.

[38] L. Rashidi, E. Vasheghani-Farahani, M. Soleimani, A. Atashi, K. Rostami, F. Gangi, M. Fallahpour, M.T. Tahouri, A cellular uptake and cytotoxicity properties study of gallic acid-loaded mesoporous silica nanoparticles on Caco-2 cells, J Nanopart Res, 16 (2014) 1-14.

[39] C. Wang, H. He, Y. Lin, L. Huang, M. Sun, T. Zhang, L. He, Preparation and preliminary application of 5-HMF@SiO_2 micro-particles, RSC Adv, 6 (2016) 70586-70591.

[40] M. Massoni, J.C.T. Clavijo, L. Colina-Vegas, W. Villarreal, J.S.M. Dias, G.A.F. da Silva, M. Ionta, M. Soares, J. Ellena, A.C. Dorigueto, M.I.F. Barbosa, A.A. Batista, Propyl gallate metal complexes: Circular dichroism, BSA-binding, antioxidant and cytotoxic activity, Polyhedron, 129 (2017) 214-221.

[41] M.S. Prevost, S. Delarue-Cochin, J. Marteaux, C. Colas, C. Van Renterghem, A. Blondel, T. Malliavin, P.J. Corringer, D. Joseph, Identification of cinnamic acid derivatives as novel antagonists of the prokaryotic proton-gated ion channel GLIC, J Med Chem, 56 (2013) 4619-4630.

[42] D. Karas, J. Ulrichova, K. Valentova, Galloylation of polyphenols alters their biological activity, Food Chem Toxicol, 105 (2017) 223-240.

[43] Z. Lu, G. Nie, P.S. Belton, H. Tang, B. Zhao, Structure-activity relationship analysis of antioxidant ability and neuroprotective effect of gallic acid derivatives, Neurochem Int, 48 (2006) 263-274.

[44] Y. Liu, K. Ai, L. Lu, Polydopamine and its derivative materials: synthesis and promising applications in energy, environmental, and biomedical fields, Chem Rev, 114 (2014) 5057-5115.

[45] K. Chen, X. Xu, J. Guo, X. Zhang, S. Han, R. Wang, X. Li, J. Zhang, Enhanced intracellular delivery and tissue retention of nanoparticles by mussel-inspired surface chemistry, Biomacromolecules, 16 (2015) 3574-3583.

[46] J. Yang, M.A. Cohen Stuart, M. Kamperman, Jack of all trades: versatile catechol crosslinking mechanisms, Chem Soc Rev, 43 (2014) 8271-8298.

[47] Y. Uekusa, M. Kamihira-Ishijima, O. Sugimoto, T. Ishii, S. Kumazawa, K. Nakamura, K. Tanji, A. Naito, T. Nakayama, Interaction of epicatechin gallate with phospholipid membranes as revealed by solid-state NMR spectroscopy, Biochim Biophys Acta, 1808 (2011) 1654-1660.

[48] H. Shadnia, J.S. Wright, Understanding the toxicity of phenols: Using quantitative structure-activity relationship and enthalpy changes to discriminate between possible mechanisms, Chem Res Toxicol, 21 (2008) 1197-1204.

[49] R. Guitard, V. Nardello-Rataj, J.-M. Aubry, Theoretical and kinetic tools for selecting effective antioxidants: Application to the protection of omega-3 oils with natural and synthetic phenols, Int J Mol Sci, 17 (2016).

[50] Y. Bai, H. Xing, P. Wu, X. Feng, K. Hwang, J.M. Lee, X.Y. Phang, Y. Lu, S.C. Zimmerman, Chemical control over cellular uptake of organic nanoparticles by fine tuning surface functional groups, ACS Nano, 9 (2015) 10227-10236.

[51] S. Kim, P.A. Thiessen, E.E. Bolton, J. Chen, G. Fu, A. Gindulyte, L. Han, J. He, S. He, B.A. Shoemaker, J. Wang, B. Yu, J. Zhang, S.H. Bryant, PubChem Substance and Compound databases, Nucleic Acids Res, 44 (2016) D1202-D1213.

[52] H. Deng, Y. Fang, Anti-inflammatory gallic acid and wedelolactone are G protein-coupled receptor-35 agonists, Pharmacology, 89 (2012) 211-219.

Figure Legends

Figure 1. Synergistic effects of gallates and magnetic force on cell-associated magnetic nanoparticles (MNPs). Gallic acid (A, B) and methyl gallate (C, D) induced a concentration-dependent increase in cell-associated MNPs (MNP_{cell}) in LN-229 (A, C) and HeLa (B, D) cells with (+) or without (-) the magnet (Mag). Values are the mean ± SE ($n = 4$). * $p<0.05$ compared to the corresponding control group. $^{\#}$ $p<0.05$ compared to corresponding values in Mag (-).

Figure 2. Gallates enhanced magnetic nanoparticle (MNP)-cell interactions and internalization. LN-229 cells were incubated with CMX-MNP (100 μg/mL; 26.32 μg/cm^2) in the presence of the vehicle (PBS; A, C), methyl gallate (30 μM; B, C), or gallic acid (30 μM; C) at 37°C or 4°C (C only) with (C only) or without the magnet for 2 h. After incubation, cells were counterstained with LysoTracker (red) for lysosomes and DAPI (blue) for nuclei (A, B). *,† $p<0.05$ compared to the corresponding groups of vehicle and gallic acid, respectively. § $p<0.05$ compared to the corresponding groups at 4°C. $^{\#}$ $p<0.05$ compared to corresponding values in Mag (-).

Figure 3. Chemical structure of gallate derivatives used in this study. The structures of gallic acid (**1**), methyl gallate (**2**), propyl gallate (**3**), gallamide (**4**), protocatechuic acid (**5**), *p*-hydroxybenzoic acid (**6**), α-resorcylic acid (**7**), trimethoxybenzoic acid (**8**), caffeic acid (**9**), dihydrocaffeic acid (**10**), and ferulic acid (**11**) are illustrated to determine the relative importance of the carboxyl or phenolic groups of gallates on cell-associated magnetic nanoparticles (MNP_{cell}). The dashed square indicates the gallic acid moiety of epigallocatechin-3-gallate (EGCG), which is the proposed pharmacophore of the effects induced by EGCG.

Figure 4. Structure-activity relationship of gallate derivatives on cell-associated magnetic nanoparticles (MNP_{cell}). LN-229 cells were incubated with MNPs (100 μg/mL; 26.32 μg/cm^2) and various gallate derivatives at 10 (A, B) or 30 μM (C, D) for 24 h in the presence (+) or absence (-) of the magnet (Mag). Values are the mean ± SE ($n = 4$). $^{*,\dagger,\S,\#}$ $p<0.05$ compared to

the corresponding vehicle (**v**), gallic acid (**1**), methyl gallate (**2**), or caffeic acid (**9**) groups, respectively.

Figure 5. DPPH radical-scavenging activity of gallate derivatives. The antioxidant activities of gallate derivatives (3~150 μM) were determined by the DPPH method at different concentrations. Values are the mean ± SE (n = 3). * p<0.05 compared to the corresponding 3 μM groups of each gallate derivative. $^{\dagger,\S,\#}$ p<0.05 compared to gallic acid (**1**), methyl gallate (**2**), and caffeic acid (**9**) groups at the same concentration, respectively.

Figure 6. Gallate derivatives exerted no cytotoxicity. LN-229 cells were incubated with the vehicle (**v**) or gallates (10 or 30 μM) in the absence (A) or presence (B) of magnetic nanoparticles (MNPs) (100 μg/mL; 26.32 μg/cm^2) for 2 h. In the presence of both gallate derivatives (30 μM) and MNPs, the effects of the magnetic field (Mag) were also evaluated (B). Values are the mean ± SE (n = 4).

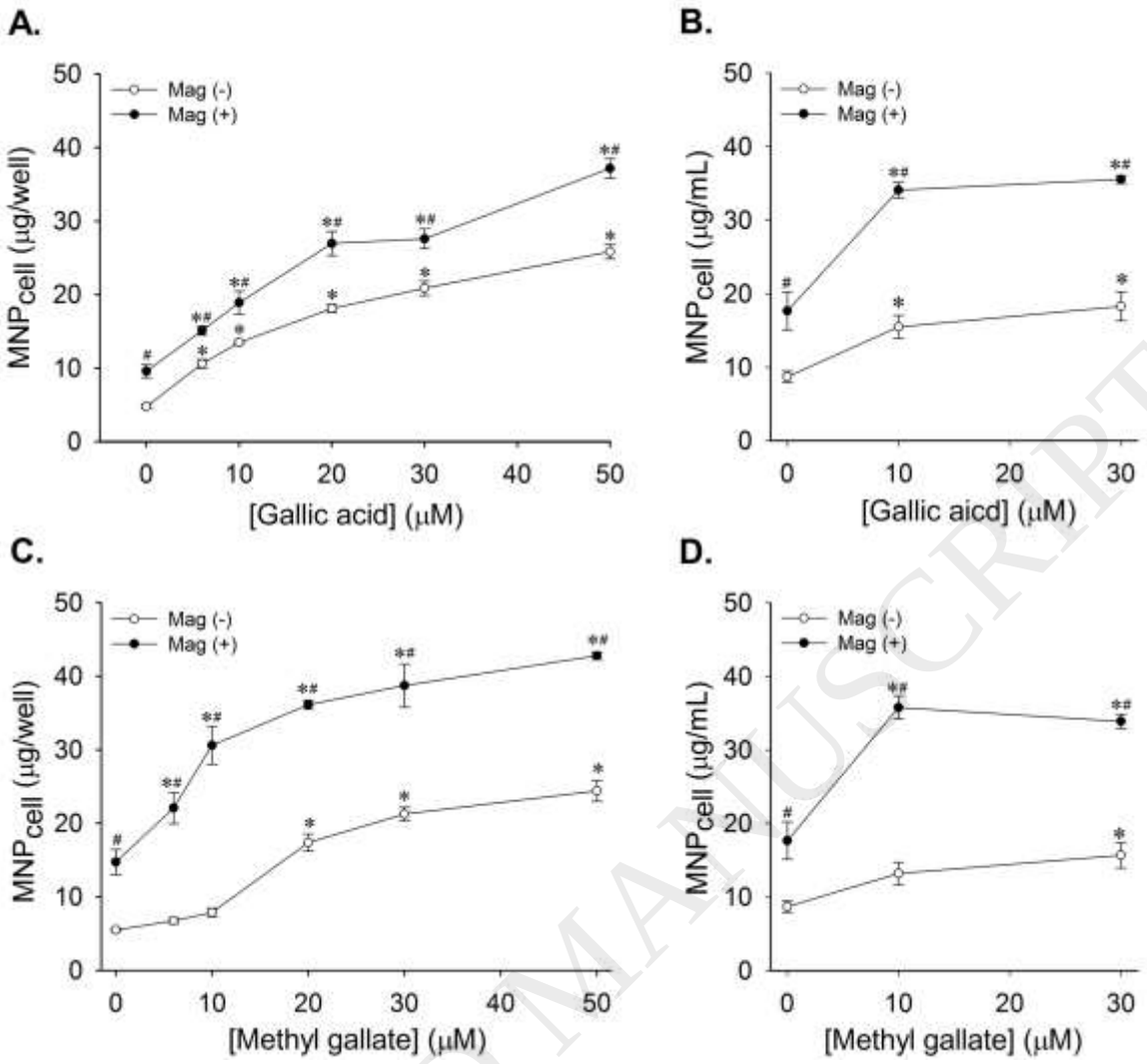

Figure 1

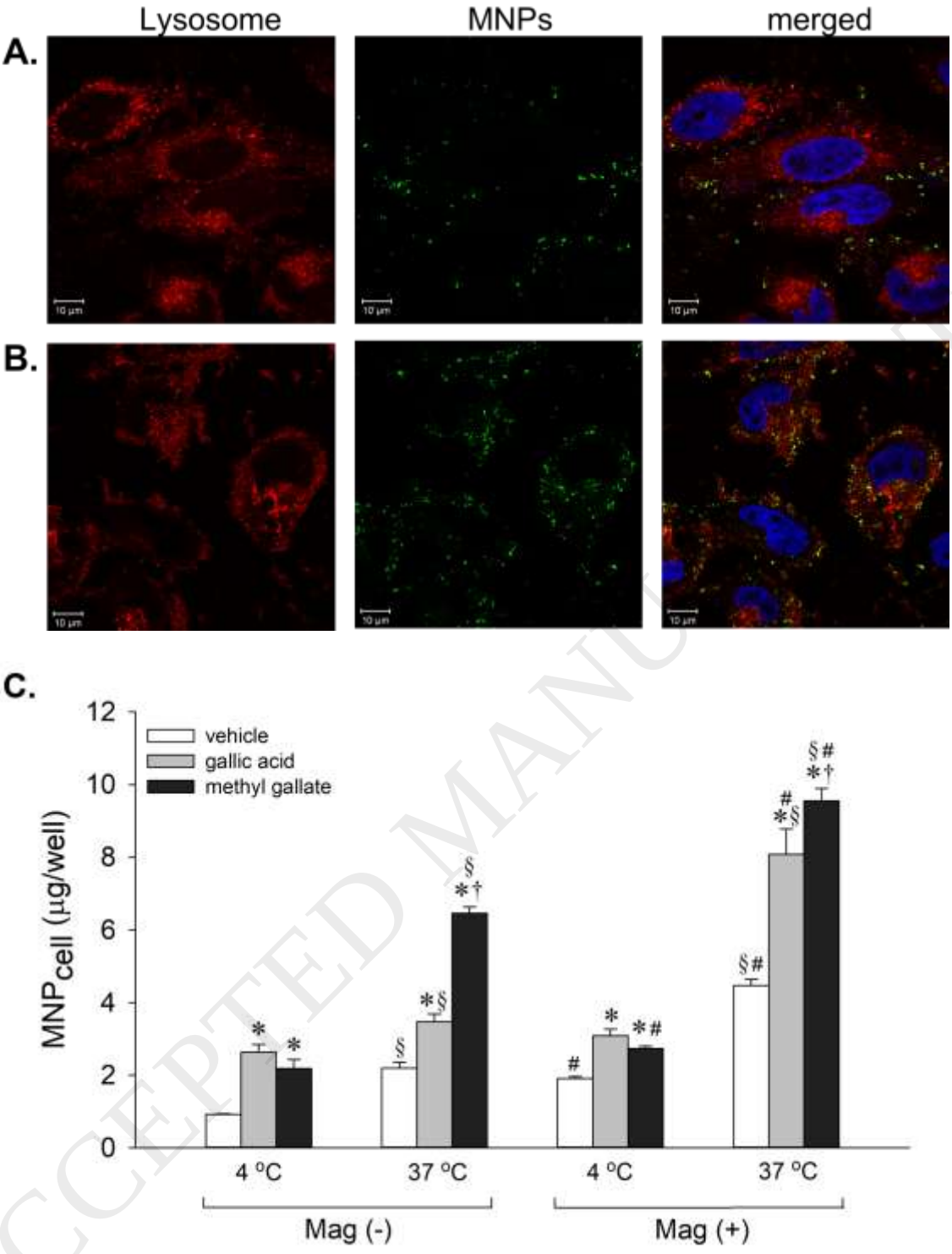

Figure 2

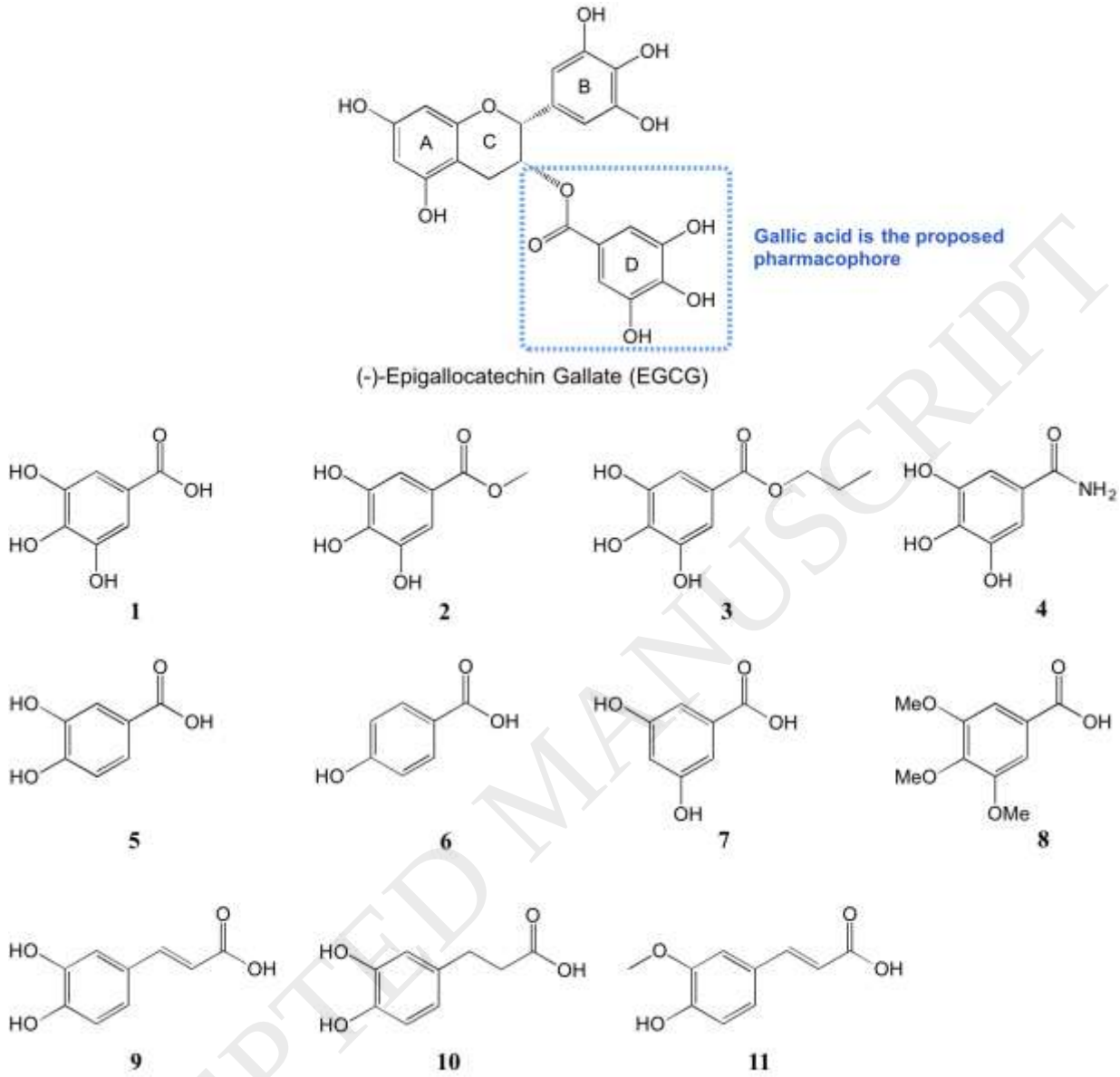

Figure 3

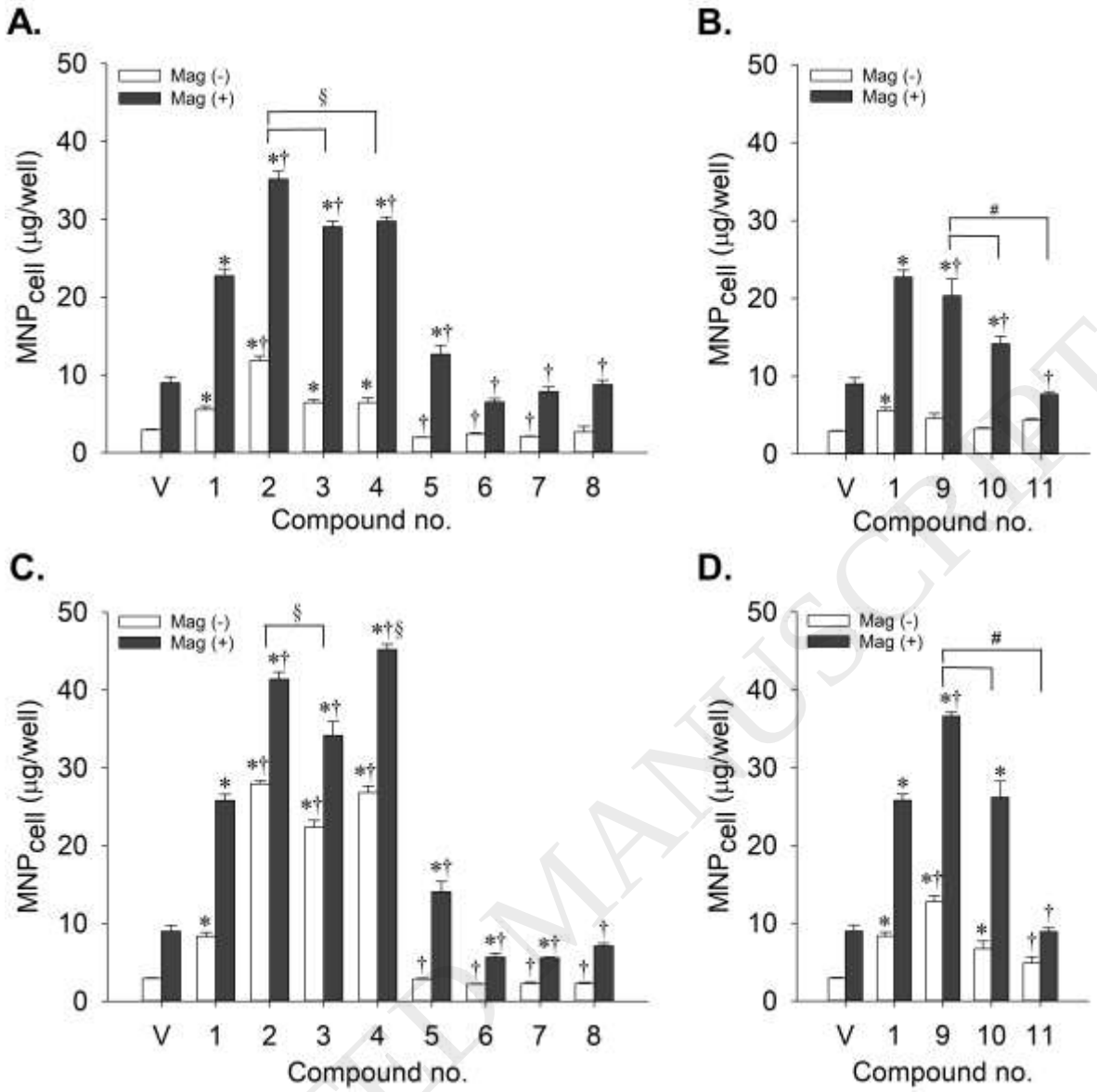

Figure 4

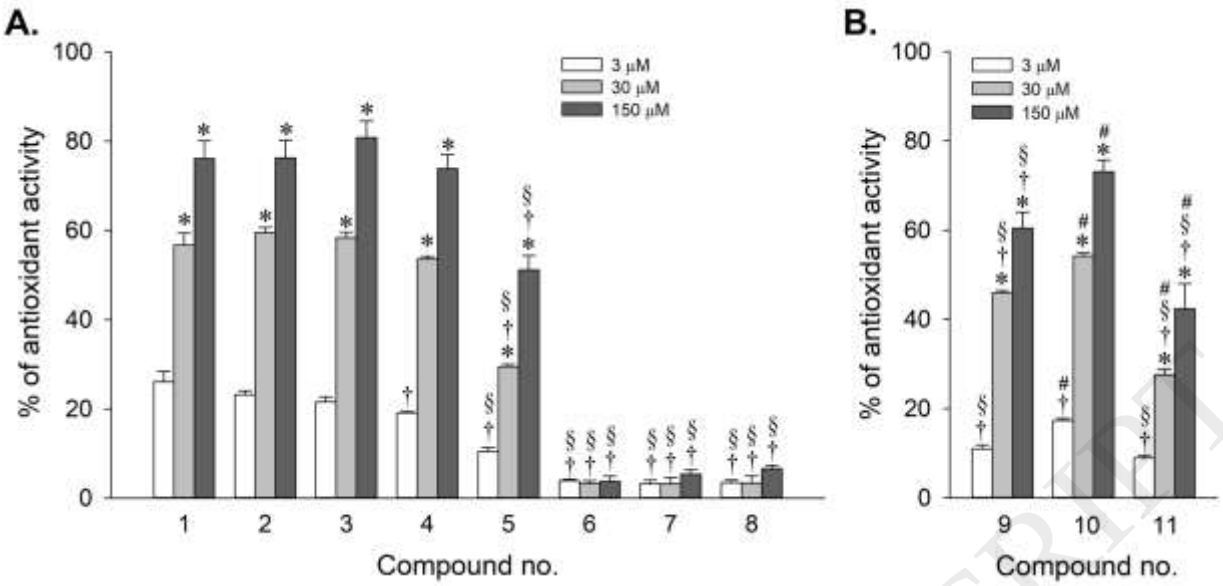

Figure 5

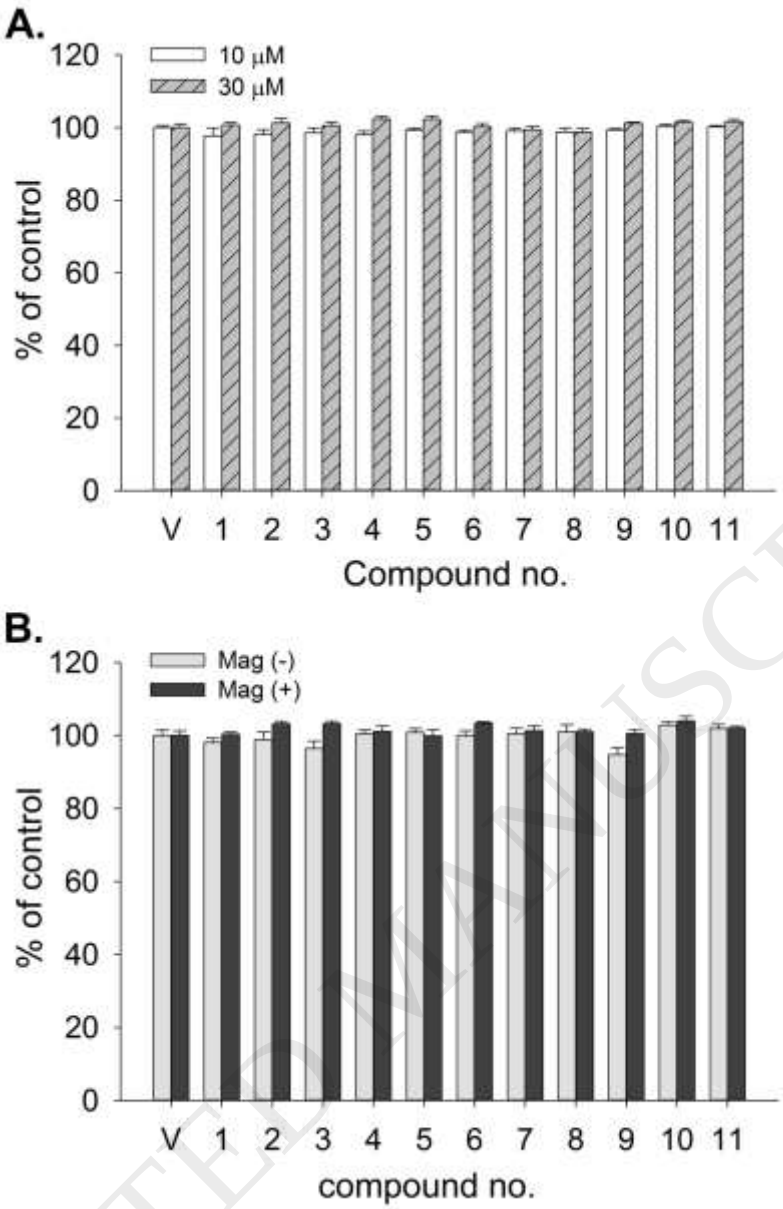

Figure 6